Communications Chemistry

https://doi.org/10.1038/s42004-026-02034-2

Article in Press

A screening strategy for vinyl acetate materials for solid-phase microextraction based on dynamic vapor sorption

Received: 28 October 2025

Accepted: 10 April 2026

Cite this article as: Niu, J., Zhao, J., Yue, L. *et al.* A screening strategy for vinyl acetate materials for solid-phase microextraction based on dynamic vapor sorption. *Commun Chem* (2026). https://doi.org/10.1038/s42004-026-02034-2

Jiajia Niu, Jichun Zhao, Liqing Yue, Wanchen Zang, Zhe Jin, Cuiliu Fu, Chen Chen, Li Dong, Youliang Zhu & Xiaojie Li

A screening strategy for vinyl acetate materials for solid-phase microextraction based on dynamic vapor sorption

Jiajia Niu[1], Jichun Zhao[3], Liqing Yue[1], Wanchen Zang[2], Zhe Jin[2], Cuiliu Fu[3], Chen Chen[1,*], Dong Li[1,**], Youliang Zhu[4], Xiaojie Li[1]

[1] Zhengzhou Tobacco Research Institute of CNTC, Zhengzhou 450001, China

[2] Jilin Tobacco Industry Company, Changchun 130000, China

[3] State Key Laboratory of Polymer Physics and Chemistry, Changchun Institute of Applied Chemistry, Chinese Academy of Sciences, Changchun 130000, China

University of Science and Technology of China, Hefei 230026, China

[4] Institute of Theoretical Chemistry, College of Chemistry, Jilin University, Changchun 130023, China

[*]Corresponding author; E-mail addresses: chenc@ztri.com.cn (Chen Chen)

[**]Corresponding author; E-mail addresses: 108591845@qq.com (Dong Li)

ABSTRACT: In solid-phase microextraction (SPME) research, selecting a coating adsorbent with good compatibility for target molecules can be difficult, and there is no specific migration testing method for vinyl acetate monomer, which is commonly used in the production of food contact materials (FCMs). First, 13 metal–organic frameworks (MOFs) with different structural characteristics and surface chemical environments were prepared and divided into three groups (good, medium, and poor) based on the dynamic vapor sorption (DVS) method. The distinction of superiority and inferiority determined by the DVS method was completely consistent with that determined by the extraction effect of the SPME probe, and the data from the two variables exhibited a statistically significant positive correlation. Then, the electrostatic potential (ESP) distribution on the typical material surface and target molecule and the charge density difference (CDD) of their interaction during adsorption were obtained using a computational simulation method. The results showed that ZIF-68 and ZIF-70 had the highest adsorption energy, which was consistent with the adsorption performance. Finally, ZIF-68 was selected as the optimal adsorption material, and the extraction conditions were optimized. The optimized method was successfully applied to test the specific migration amounts of several ethylene vinyl acetate (EVA) copolymer materials.

Keywords: SPME, MOF, Vinyl acetate, Ethylene vinyl acetate (EVA), specific migration

1. Introduction

It is important to study the migration of contaminants and other harmful components from food contact materials (FCMs) to food or food simulants. The residual amount represents the content of a component in the object (many components are highly solidified or tightly bound to the substrate, which makes them difficult to extract). The migration amount can be objectively used for the quality and safety risk assessment of the material or product. Therefore, the regulation of restricted substances in FCMs within the EU, China, and other countries has shifted from controlling residual amounts to controlling the migration amounts[1,2]. In addition, increasingly many researchers are interested in determining the migration amount of organic or inorganic pollutants. For example, Wenjuan Zhu et al. established a green extraction and determination method for analyzing the migration of antioxidants from plastic packaging materials into food simulants[3]. According to EU technical standard EN13130-1:2004 (E), Meigui Xue et al. simulated the migration of pollutants from paper to powdered food using type-E artificial migration cell, and the specific migration amount/rate of the pollutant was detected using GC-MS[4]. Michaela Lerch et al. investigated the specific migration of three per- and polyfluoro alkyl substances (PFASs) from six FCMs into food or food simulants (50% and 20% ethanol) under high-temperature conditions[5]. Vinyl acetate is primarily used as a monomer in the production of ethylene vinyl acetate (EVA), polyvinyl acetate, polyvinyl alcohol, etc., which are widely used in the coating of FCMs, plastic products, adhesives. However, because of the incomplete polymerization, low levels of vinyl acetate molecules are present in FCMs, which pose a risk of migrating into foodstuffs and eventually entering the human body. According to Regulation (EC) No. 1935/2004[1] and the latest instructions on plastics[2], coatings, and

other FCM products, the specific migration limit (SML) of vinyl acetate is 12 mg·kg^{-1}. Vinyl acetate is an irritant to human skin, the upper respiratory tract, and eyes, and it also acts as a central nervous system depressant[6]. The WHO's International Agency for Research on Cancer (IARC) ranked vinyl acetate as a Group-2B carcinogen in 2017[7]. Therefore, it is very important to determine the specific migration of vinyl acetate for the risk assessment of vinyl acetate in FCMs.

The current determination of vinyl acetate mainly focuses on trace residues in packaging materials, and the main test method is headspace gas chromatography (HS-GC)[8]. The specific migration testing method for vinyl acetate has been rarely reported. If the specific migration of organic monomers in other FCMs is used as a reference, GC-MS, high-performance liquid chromatography (HPLC), and liquid chromatography-mass spectrometry (LC-MS) are commonly used[9, 10]. However, food simulants often require intensive extraction and enrichment before they can be detected by instruments, so a simple and feasible in-situ detection method must be developed.

Solid-phase microextraction (SPME) is a sample pretreatment method based on adsorption extraction and pre-concentration. The concentration balance of the target analyte is reached between the sample and the adsorbed phase, and the analyte content is determined by the detector after desorption[11]. The SPME technique has the advantages of simple operation, a low sample loading, and a high enrichment factor. The probe coating is the key to achieve good extraction effect of the SPME analysis method. Commercially available SPME probes mainly include polymer coatings (such as polydimethylsiloxane and polyacrylate) and carbon-doped polymer coatings (such as polydimethylsiloxane/carbon and polydivinylbenzene/carbon), but they have poor thermal stability and poor mechanical properties of quartz carriers. Therefore, developing SPME probes with a high enrichment coefficient, good selectivity, and good mechanical properties is an important development direction in SPME research. Recently, a series of new coating materials has been developed, such as graphene[12], carbon nanotubes[13, 14], covalent organic frameworks[15, 16], molecularly imprinted polymers[17, 18], aerogels[19, 20], and ionic liquids[21, 22], which have promoted the development of this field.

Metal–organic frameworks (MOFs) are composed of inorganic centers and organic ligands connected by coordination bonds[23, 24] and have high thermal stability, easy tuning, and large specific surface areas, which make them attractive coating materials for SPME. Cui et al. first reported the use of MOF-199 as a coating for SPME in 2009 to extract benzene homologues of volatile harmful substances[25]. Then, Fe-BDC, UiO-66, and MIL-type MOFs were successively developed into SPME materials[13, 26, 27]. Recently, Mondal et al. prepared the MIL-101(Cr)-NH_2-coated SPME probe to detect six antibiotics across four classes of tilapia[28]. Serkan Bolat et al. reported that MOF-801 was coated onto a stainless-steel wire to prepare an SPME probe, and the probe was then introduced into a Tedlar bag that contained an analyte under steady-state condition. Benzene, toluene, ethylbenzene, and xylene (BTEX) were analyzed[29]. The above research indicates that valuable studies have been conducted focusing on the enrichment and analysis of organic and inorganic pollutants, with MOFs being used as candidate materials for SPME coatings.

The adsorption material in the probe coating is the core of the SPME technology. However, there has been no reliable method to accurately predict the adsorption effect between coating material and target molecule or their adsorption compatibility in previous research. The selection of adsorbent materials for specific targets is also slightly less purposeful, and the adsorption mechanism has not been deeply explored. In this context, the density functional theory (DFT) is an effective approach. DFT is an approximate method to address multi-atomic systems based on atomic simulation, and it can provide a deeper understanding of the structure and chemical properties of materials[30, 31].

In this paper, a dynamic vapor sorption (DVS) method was established to screen the adsorption capacity of 13 MOFs for vinyl acetate. In situ polymerization of polyamide acid was used to prepare an SPME probe, with a coating of MOF/PI composite on a stainless-steel wire carrier[32]. The consistency of the good, medium, and poor groups of those materials between the DVS method and the SPME method was verified (Figure 1(a)). Based on the computer simulation, the electrostatic potential (ESP) distribution on the surface of materials and target molecules was obtained, the nucleophilic or electrophilic property of the molecular surface was determined, and the interaction between target molecule and specific groups of the adsorption material was analyzed. In the DFT framework, the distribution of electrons can be approximated by solving the Schrödinger equation, and the adsorption energy between vinyl acetate and different MOF materials can be obtained, which can reveal the adsorption mechanism of vinyl acetate molecules on the surface of MOFs from a molecular perspective. ZIF-68 was selected as the coating material for the SPME testing of vinyl acetate. The extraction conditions (salt concentration, temperature, rotation speed, and extraction time) were optimized. Finally, the method was applied to test the specific migration of vinyl acetate in materials such as food packaging films, EVA coatings, and infusion bags (Figure 1(b)).

2. Methods

2.1 Reagents and materials

4,4'-Diaminodiphenyl ether (98%), pyromelliticdianhydride (99.5%), 3,3',4,4'-benzophenonetetracarboxylicdianhydride (99%), N,N-dimethylformamide (99.8%), P-phenylenediamine (99%), 3,3'-diaminobenzophenone (TCI, >95%),4,4'-diaminodiphenyl ether (98%), and vinyl acetate (99%) were purchased from the Beijing J&K Technology Co., Ltd. (Beijing, China). Sodium chloride (AR) was purchased from Tianjin Chemical Reagent Factory No. 3. Deionized water was prepared using Sartorius H_2O-MM-UV-T (Gottingen, Germany). Methanol (GR) and ethyl alcohol (GR) were purchased from Sinopharm Chemical Reagent Co., Ltd. (Shanghai, China). Food vacuum packaging compression film (EVA food storage bag, Tianmeiqi Flagship Store, hereafter referred to as food packaging film), food contact material coating (Yike Packaging Products, hereafter referred to as EVA coating), and nutrient solution infusion bag (EVA nutrition infusion bag, Hongying Medical Devices Specialized Store, hereafter referred to as infusion bag) were obtained from TaoBao online. Additionally, a 20-mL headspace bottle was purchased from the Shanghai Anpu Experimental Technology Co., Ltd. (Shanghai, China) and 5-μL microliter syringes were obtained from the Shanghai Gaoge Industrial and Trading Co., Ltd. (Shanghai, China).

2.2 Instrumentation

Powder X-ray diffraction (PXRD) detections were performed on a Bruker D8 ADVANCE X-ray powder diffractometer (Cu target wavelength: 1.5406 Angstroms; tube current: 40 mA; tube voltage: 40 kV; rate: 6°·min^{-1}). Nitrogen (N_2) adsorption/desorption experiments were performed on a Micromeritics ASAP 2460 gas adsorption analyzer (the degassing conditions were as follows: 200°C for 4 h; adsorbed gas: N_2; temperature: −77 K) (Micromeritics, USA). The scanning electron microscope (SEM) images were obtained using a Hitachi S-4800 scanning electron microscope. DVS detections were performed on DVS analyzer (Beijing BSD-DVS Instrument Technology Co., Ltd.). Other instruments used in this study were as follows: a Sartorius CPA225D balance (accurate to 0.00001 g), a temperature controlled magnetic stirrer (TALBOYS), an agitator (Shanghai Aladdin Biochemical Technology Co., Ltd.), an oven (Shanghai Yuejin Medical Equipment Factory (101-1-BS), stainless-steel wire (Shenzhen Kanghong Metal Products Co., Ltd., 304 stainless steel wire, diameter: 0.1 mm), and a Calvet-type micro-calorimeter (C80, Setalam Instruments, France).

All analytes were examined using an Agilent 6890B equipped with a split/splitless injector, a flame ionization detector (FID), and a DB-624 capillary column (60 m × 0.32 mm i.d. × 1.8 μm) (California, USA).

2.3 Preparation of materials and homemade probe

Initial screening materials: Based on their good thermal stability, excellent water resistance, and large specific surface area, while taking into account randomness and extensibility, we selected and prepared the following 13 MOFs: CAU-1-NH_2, MIL-53(Cr), ZIF-8, MIL-53(Al), PCN-250(Fe), UIO-66-COOH, UIO-66, CAU-10, UIO-66-NH_2, MIL-101(Al)-NH_2, MOF-74, MOF-199, and MIL-53(Al)-NH_2 (Table S1 1–13 show the structures). These materials were prepared referring to the reported method presented in the Supplementary Information Section 2.2.

Synthetic Procedures for ZIF-68: The synthetic method comprised the following steps. First, in a 20-mL headspace vial, 2-nitroimidazole (0.72 mmol), benzimidazole (0.24 mmol), and zinc nitrate (0.24 mmol) were completely dissolved in 6 mL of a mixed solvent of N, N-dimethylformamide and N, N-diethylformamide (1:1), sealed, and reacted at 100°C for 72 h. The product was sequentially cleaned with N, n-dimethylformamide, ethanol, and methanol. Then, it was soaked in methanol for 12 h and vacuum-dried at 80°C for 12 h for later use.

Further research materials included ZIF-68, ZIF-70, ZIF-11, ZIF-90, and ZIF-67 (Table S1 14–18 show the structures), which were prepared referring to the method presented in Supplementary Information Section 2.3.

The SPME probes (13 initial screening materials and 5 further research materials) were prepared by controlling the coating material mass to ~1.0 mg according to the polyamide acid (PAA) heating-curing method. By preparing 3–5 parallel samples per needle, we varied the coating amount. The SPME probe with the coating amount closest to 1.0 mg was selected and heated to form the probe[32]. Then, the SPME probe/fiber was loaded into a modified 5-μL high Gaoge injection needle (see Figure S2 in the Supplementary Information for the homemade probe). Supplementary Information Section 4 shows the PI coating blank experiment.

2.4 Experimental method for compatibility screening and the investigation of adsorption properties

2.4.1 DVS method

The largest adsorption of MOFs was determined based on the dynamic vapor sorption.

The material activation conditions were as follows: activating temperature: 150°C; activating time: 3 h; degassing method: atmospheric purge. Taking UiO-66-COOH as an example, Section 5.3 of Supplementary Information shows the sample mass change curve during the activation process. The quality curve gradually stabilized, which indicates that the activation was complete.

The adsorption capacity was determined under the following conditions: the atmosphere gas was a mixture of 10% vinyl acetate/nitrogen, the adsorption temperature was 30 °C, and the adsorption equilibrium condition was considered to be equilibrium with a fluctuation of ± 0.1 mg/60 min. The total atmospheric gas flow rate was 400 SCCM (the total amount of gas flowing through the sample surface per minute under standard conditions).

2.4.2 Probe method

The target molecules were extracted via headspace-solid phase microextraction (HS-SPME). A 5-mL 10.0-μg·mL^{-1} aqueous standard solution of vinyl acetate was transferred into a 20-mL headspace vial. The headspace vial contained a magnetic stir bar and was placed in a water bath using a temperature-controlled magnetic stirrer. The extraction temperature was controlled by adjusting the water bath temperature. Subsequently, the extraction performance of the prepared SPME probe was evaluated using gas chromatography inlet thermal analysis, chromatographic column separation, and FID detection.

HS-SPME conditions: extraction temperature: 30°C; extraction time: 15 min; salt concentration: 30%; agitation speed: 600 rpm.

GC conditions: inlet temperature: 230 °C; shunt ratio: 5:1; flow: 2 mL·min^{-1}; injection time: 30 s; column: DB-624, 60 m × 0.32 mm × 1.8 μm.

Heating procedure: the temperature was first maintained at 40°C for 3 min and subsequently increased to 230 °C at 10 °C·min^{-1} in 5 min.

2.5 Adsorption mechanism

DFT calculations were performed to elucidate the adsorption mechanism of vinyl acetate on different MOF surfaces. All DFT calculations were performed using the Vienna Ab initio Simulation Package (VASP)[33]. To ensure calculation accuracy and reduce computational complexity, we used a Cluster structure to describe the MOFs and Vaspkit tools to aid the DFT computations[34]. To balance the computational accuracy and efficiency, cluster models were used to represent the MOFs. The clusters were constructed as representative local structural units that were extracted from the corresponding periodic frameworks to preserve the original coordination environments of the metal nodes. In the present work, all MOF clusters consisted of one metal node, which was coordinated by four ligands, and all dangling bonds at the cluster boundary were saturated with hydrogen atoms to remain chemically stable. For each MOF–VA system, several initial adsorption configurations were examined, and the structure with the lowest total energy after optimization was used for subsequent analyses. To process the results, the VMD software was applied to obtain ESP distribution maps of the molecular surfaces, while the VESTA software was used to visualize the charge density difference (CDD) during the adsorption process[35, 36], and adsorption energies were calculated based on the energy differences before and after the adsorption of vinyl acetate onto the MOFs. The calculation method and formula are presented in Supplementary Information Section 7.

2.6 Optimization of the HS-SPME extraction procedure

The performance of the SPME probe is affected by the type of adsorbed material, salt concentration, temperature, agitation speed, extraction time. In this experiment, a 0.1-μg·mL^{-1} vinyl acetate standard solution was first prepared, and 5.0 mL of the solution was transferred into a 20-mL headspace vial as the test sample. The best extraction conditions were successively optimized according to the above-mentioned parameters. The GC conditions were identical to those in Section 2.4.2.

2.7 Real sample test

Food packaging film, EVA coating, and infusion bag were tested. Migration tests were performed using 10% ethanol, deionized water, and normal saline as the simulation liquids at ratios of 6 dm^2 in contact with 1 kg of the simulated substance(6 cm in width and 10 cm in length of food packaging film, infusion bag, and 60 cm^2 EVA coating, added 100 mL simulated substance). The migration condition was as follows: soaking at room temperature for 7 days or 40°C for 30 min. The sample was prepared by adding 0.5 mL soaking solution to 4.5 mL deionized water. In accordance with the sample solution matrix, a standard solution of the required concentration was prepared. With butyl acetate as the internal standard, we determined the migration quantity and recovery rate of vinyl acetate in the sample. The instrument parameters were identical to those in Section 2.4.2, and Table 1 shows the extraction conditions.

3. Results and discussion

3.1 Characterization of MOF materials and homemade probe

The morphological characteristics and structures of the 13 materials (used in the initial screening) and 5 materials (used in further research) were analyzed by SEM and X-ray diffraction (XRD). We use the ultimately selected ZIF-68 adsorption material as an example. As shown in Figure 2-1, the particles of the ZIF-68 sample were uniform, and they formed a hexagonal prismatic crystal structure with approximate dimensions of 9 μm × 2.5 μm. Figure 3 (the source data can be found in Supplementary Data 1) shows the XRD pattern of ZIF-68. The XRD pattern of ZIF-68 was consistent with the theoretical simulation spectrum, which indicated that the prepared adsorption material was pure-phase and had good crystallinity.

Supplementary Information Figure S1, Table S2 and Table S3 of Section 2.2, and Table S4 of Section 2.3 show the SEM and XRD results for the other materials.

The test result of the BET surface area is shown in Table S2 in the Supplementary Information. The adsorption data show that 13 MOFs had good adsorbability for N_2, which had established a favorable spatial foundation for the extraction of vinyl acetate.

The SEM results of the homemade probe (Figure 2-2) showed that the ZIF-68 coating material formed a uniformly thick film on the surface of the steel needle; the thickness was approximately 80 microns.

3.2 Compatibility screening and investigation of adsorption properties

No previous studies have reported on suitable coating materials and the adsorption compatibility of different materials with vinyl acetate target molecules. The conventional characterization test of N_2 adsorption can provide the adsorption possibility or space size of the material, but the compatibility "value" of the internal environment of the material with the target molecule is unknown. Thus, we designed a DVS method for the primary screening of materials. The principle (see Figure S4 in the Supplementary Information for the schematic diagram) involves exposing the activated material to a specific concentration of vinyl acetate gas (with nitrogen as the dilution gas). The adsorption value of the material for vinyl acetate is calculated using the weight difference method after reaching the adsorption equilibrium, and the adsorption mass number of vinyl acetate per unit material mass is reported. The DVS curve shows large disparities in the adsorption rate and the maximum adsorption amount of vinyl acetate among the selected adsorption materials (Figure 4(a)) (the source data as shown in Supplementary Data 2). The maximum adsorption capacity can be divided into three groups: good (greater than 300 $mg \cdot g^{-1}$, classified as a group with potential), medium (100–300 $mg \cdot g^{-1}$, classified as a group with moderate effect), and poor (less than 100 $mg \cdot g^{-1}$, classified as a group with poor effect) (Figure 4(b)). The adsorption rate of materials with different adsorption effects also varied. In general, the material with good adsorption effect more quickly reached the saturation state, the material with slightly poor adsorption effect took a longer time to saturate, and the material with extremely poor adsorption effect had difficulty reaching saturation.

Accordingly, the SPME probes were coated with equal mass of different materials as the validation group. Figure 4(c) shows the test results on the adsorption properties of vinyl acetate. Based on the classification outlined in Figure 4(b), we conducted SPME tests on the materials within each of the three groups. As shown in Figure 4(c), the SPME performance of the materials in the "good" group was significantly higher than those in the "medium" and "poor" groups. Two materials exhibiting moderate SPME performance were observed in the "medium" group, whereas all four materials in the "poor" group demonstrated low performance. The ratio of the average GC signal values among the three groups in the probe test were 35.4:4.4:1, whereas the corresponding average adsorption capacity ratios in the DVS group were 16.4:9.6:1. Furthermore, we quantified and evaluated the linear relationship between the DVS adsorption capacity of 13 materials and the peak area of SPME. The Pearson correlation coefficient (r) was 0.8038 (p=9.29E-4) (The results of the linear regression fitting are presented in Supplementary Information Figure S6). After excluding the 4 materials (PCN-250(Fe), UiO-66-COOH, CAU-10, MOF-74) whose SPME test results were close to 0 and had no dose-effect relationship, the "r" of the 9 groups of data increased to 0.9358 (p=2.07E-4) (The results of the linear regression fitting are presented in Supplementary Information Figure S7). These results indicate that: 1) under SPME or DVS conditions, the distinctions among the three groups are highly evident. 2) the SPME and DVS methods are fully consistent in terms of the qualitative identification and classification of the three main categories, i.e., "good," "medium," and "poor;" 3) as can be seen from the Pearson correlation coefficient (r), there was a strong positive linear correlation between the DVS and SPME data, and 4) the DVS method was used to determine the amount of vinyl acetate adsorbed by the material under a certain ratio of vinyl acetate vapor to nitrogen pressure (P/P_0), while the SPME probe extraction is based on the three-phase equilibrium among the aqueous phase, headspace phase, and SPME probe phase. These represent different extraction environments compared to those used in the DVS method. Hence, the DVS and SPME methods did not yield identical rankings of materials within each group. Overall, both methods demonstrated high effectiveness. Notably, the DVS method offers the added advantage of simplicity, making it a particularly promising approach for the preliminary screening of potential SPME coating materials.

All 13 materials had large specific surface areas and accessible windows/pores but different extraction effects of SPME. MIL-53(Cr) and MIL-53(Al) appeared to be effective due to their matching morphology. ZIF-8, which was constructed from conjugated or aromatic N atoms, also had a good adsorption driving force, whereas the -NH_2 groups, which were modified on the benzene ring, did not generate this driving force. MIL-53(Al) significantly decreased after being modified by NH_2. Because conjugated or aromatic N atoms had an effective driving force, the screening range of ZIF series materials was expanded. Several materials such as ZIF-67, ZIF-70, ZIF-11, ZIF-90, and ZIF-68 were synthesized, and the SPME probes of these materials were prepared to compare their extraction effects. As shown in Figure 4(d), ZIF-68 and ZIF-70 were significantly improved. The reason may be that their unique nitro group has generated another adsorption driving force, so the conjugated or aromatic N atom with a nitro group generated a double driving force and made ZIF-68 and ZIF-70 exhibit the best SPME effect. The adsorption enthalpy of ZIF-68 for vinyl acetate was determined to be −31.96 $kJ \cdot mol^{-1}$ using microcalorimetry (see Section 6 in the Supplementary Information). The results indicate that the primary adsorption interactions were van der Waals forces and hydrogen bonding. Since these intermolecular forces were consistent across both the DVS system (gas-to-material) and the SPME system (aqueous-to-gas-to-material), this observation confirms the correlation between gas-phase adsorption capacity in DVS and liquid-phase extraction efficiency in SPME.

3.3 Discussion of adsorption mechanism

To save time and resources, representative and promising MOFs, ZIF-8 and MIL-53 (including the later-discovered better materials ZIF-68, ZIF-70, and MIL-53 with group transformation), were selected from the "good" group for computational simulation, with the aim of studying the adsorption mechanism of vinyl acetate on the surface of MOFs from a molecular perspective. To identify the adsorption sites of vinyl acetate and these MOFs, it is necessary to first understand the ESP distribution on the surface of these molecules and subsequently determine the nucleophilic or electrophilic characteristics of the molecule surface groups. Figure 5 (the source data can be found in Supplementary Data 3) shows the ESP distribution maps and its extreme values of vinyl acetate, MIL-MOFs, and ZIF-MOFs. The red part was ele

ctron-rich and had nucleophilicity; the blue part was electron-poor and had electrophilicity, the cyan and green markers denote the surface ESP minima and maxima, respectively, and the corresponding values are labeled beneath each panel. Figure 5(a) shows the ESP distribution of vinyl acetate molecules. Carbonyl O has obvious nucleophilicity with abundant electrons, whereas the methyl group and vinyl have obvious electrophilicity without electron (the methyl group had stronger electrophilicity, with a maximum ESP value of 63.6 kcal/mol). Figures 5 (b–f) show the ESP distributions of MIL-53 (Al), MIL-53(Al)-NH_2, ZIF-8, ZIF-68, and ZIF-70. The MOFs containing oxygen atoms formed a nucleophilic region near O, whereas the benzene rings and conjugated structures containing N protons tended to form a positively charged region with strong electrophilicity. In comparison, ZIF-MOFs exhibited more pronounced ESP extrema. Notably, ZIF-8 had strong positive ESP regions, which were associated with conjugated N atoms, and relatively weak negative ESP regions. In contrast, ZIF-68 and ZIF-70 exhibited both strong positive and negative surface potentials because conjugated N atoms and nitro groups coexisted.

Based on the ESP distributions and surface extrema, we identified plausible adsorption sites for vinyl acetate on the MOFs by considering the electrostatic complementarity between oppositely charged regions. In particular, the nucleophilic carbonyl O atom of vinyl acetate should favorably interact with electrophilic conjugated N sites on ZIF-MOFs, whereas the electrophilic methyl group of vinyl acetate might interact with electron-rich regions associated with nitro groups. These ESP-guided considerations were used to construct the initial adsorption configurations for subsequent geometric optimization and adsorption energy calculations.

The obtained adsorption energies can be used to compare the adsorption strength between vinyl acetate and the aforementioned MIL-MOFs and ZIF-MOFs. As shown in Figure 6(a), the adsorption energies of ZIF-70, ZIF-68, ZIF-8, MIL-53(Al), and MIL-53(Al)-NH_2 were −53.1, −50.7, −40.1, −38.3, and −35.4 kJ/mol, respectively. The higher adsorption energy indicates that more energy was released during the adsorption process, which was conducive to the interaction, and the adsorption amount increased. The lower adsorption energy indicates poor compatibility and reduced adsorption capacity. In general, ZIF-MOFs had higher adsorption energy for vinyl acetate than MIL-MOFs, and ZIF-70 and ZIF-68 had significantly stronger adsorption energy than the other materials.

What causes the disparity in adsorption energy? To reveal the underlying mechanism, the charge redistribution during adsorption was analyzed using CDD maps and Bader charge analysis. Figures6 (b–d) show the molecular association results. In the CDD diagram in Figures 6(b–d) (the blue area indicates a decrease in charge density, and the yellow area indicates charge accumulation), compared to the MIL-MOFs, the ZIF-MOFs exhibited more significant charge redistribution during adsorption. In Figure 6(b), the carbonyl group, methyl group, and vinyl group of vinyl acetate interacted with the alkyl, nitro, and conjugated N-atoms of ZIF-70 and ZIF-68, respectively, which significantly changed the charge density before and after adsorption. In particular, all three atoms on the nitro group showed local charge density changes, which indicates that the intermolecular binding was closer. ZIF-8 (Figure 6 (c))

had a weaker change in charge density than ZIF-70 and ZIF-68 due to the lack of nitro group. However, in Figure 6 (d), the interaction between MIL-MOFs and vinyl acetate during adsorption only occurred between the O atom, benzene ring, methyl group, and the vinyl group of vinyl acetate on MOFs, which slightly changed the charge density. In particular, MIL-53(Al)-NH_2, due to the introduction of amino groups at the benzene intersite, had a strong hydrogen bonding effect that narrowed the pore structure[37] , which might have caused its poor adsorption effect for vinyl acetate.

To quantitatively compare the electronic response during adsorption, the absolute change in net Bader charge of the vinyl acetate molecule (|Δq|) was calculated for each adsorption system. The results show that the |Δq| values for vinyl acetate adsorbed on ZIF-MOFs were approximately one order of magnitude larger than those for vinyl acetate adsorbed on MIL-MOFs, which indicates a much stronger degree of charge redistribution and electronic polarization during adsorption. Although the adsorption energies moderately differed, the significantly larger charge rearrangement suggests that ZIF-MOFs induced more substantial electronic interactions with vinyl acetate. Figure S9 in Supplementary Information Section 7.2 shows an additional structural evidence, which summarizes key intermolecular distances in the optimized adsorption configurations. In ZIF-68 and ZIF-70, the distances between O atoms in the nitro groups and H atoms of the vinyl acetate methyl group were shorter than 2.3 Å. In addition, the H atoms that bonded to conjugated N atoms or adjacent methylene groups in the ZIFs exhibited short distances to the carbonyl O atom of vinyl acetate. These close contacts sharply contrast with the larger intermolecular separations observed in MIL-MOFs, which supports the enhanced interaction between vinyl acetate and ZIFs that contained both conjugated N atoms and nitro groups.

Based on the above results of the adsorption energies and charge transfer distribution, the selection of ZIF-68, ZIF-70, or other MOFs containing conjugated N atoms and nitro structure would obtain a more effective adsorption effect for vinyl acetate, which explains their best effect as probes.

3.4 Optimization of the SPME extraction procedure

3.4.1 Optimization of the salt concentration

The addition of salt in the water phase affected the ionic strength of the substrate and subsequently affected the partition coefficient of the target substance for the substrate, headspace, and coating. The effects of the sodium chloride concentrations (10%, 20%, 30%, and 36%) on the extraction effect were investigated, as shown in Figure 7 (a). With the increase in sodium chloride concentration, the extraction effect almost linearly increased. The SPME extraction maximized at 30% salt concentration. When the solubility of sodium chloride in water reached saturation, the extraction effect decreased, so the 30% salt concentration was selected as the best salt concentration.

3.4.2 Optimization of the extraction temperature

The extraction temperature greatly affected the diffusion of vinyl acetate from the aqueous phase to the headspace phase. An appropriate temperature was conducive to the diffusion of analytes from the solution to the headspace phase. Low temperature did not benefit the movement of vinyl acetate molecules, making it difficult to enter the headspace phase from the aqueous phase; however, if the temperature was too high, the vinyl acetate molecules easily desorbed from the coating material. Therefore, it is necessary to find the temperature that can not only form an effective concentration in the headspace phase but also maximize the retention on the adsorbing material. The extraction effects of the ZIF-68 SPME probe for vinyl acetate at 2°C, 5°C, 10°C, 20°C, 30°C, and 40°C were investigated. As shown in Figure 7 (b), the extraction effect gradually improved with the increase in temperature, and the best extraction effect was obtained at 10°C.

3.4.3 Optimization of the agitation speed

Stirring could accelerate the transfer of substrate, and increasing the stirring speed could enhance the diffusion of analyte from the sample solution to the headspace phase, which increased the analyte concentration around the SPME probe and the extraction efficiency of the sample. As shown in Figure 7 (c), with the increase in stirring speed, the extraction efficiency increased markedly. When the stirring speed was 800 rpm, the best extraction effect was obtained. If the stirring speed continued to increase, the extraction effect no longer improved, so 800 rpm was selected as the optimal stirring speed.

3.4.4 Optimization of the extraction time

With extended extraction time, the adsorption amount of the adsorbed material for the target molecule gradually reached the adsorption saturation state. The adsorption amount did not increase if the extraction continued, and desorption from the material occurred. The extraction time of 5, 10, 15, 20, 25, and 30 min was investigated. As shown in Figure 7 (d), the adsorption capacity maximized when the extraction time was 20 min; when the extraction

time extended to 25 min, the adsorption capacity slightly increased. When the extraction time was 30 min, the desorption process dominated, and the adsorption capacity decreased. Considering the experimental efficiency, 20 min was selected as the extraction time for subsequent experiments.

The single-factor conditions were optimized in four aspects: salt concentration, extraction temperature, stirring speed, and extraction time. Table 1 shows the optimization results.

3.5 Characteristic parameter analysis

The extraction performance of the prepared ZIF-68 SPME probe on vinyl acetate was investigated and Table 2 shows the experimental results. Different concentrations of standard solution (0.001–10 μg·mL^{-1}) were prepared, and the linear correlation was determined. The coefficient of determination (R^2) was 1.00 based on linear fitting, which indicates a good linear relationship. The detection limit of the method was 0.0001 μg·mL^{-1} based on the triple signal-to-noise ratio. The experiment was repeated five times with 0.1 μg·mL^{-1} vinyl acetate, and the repeatability RSD was 7.6%, which indicates good repeatability. The lifetime of the ZIF-68-coated SPME probe was more than 200 times (The results of residual assessment, method precision and lifetime assessment method can be found in Section 8 of Supplementary Information).

The detection limit of the SPME probe prepared with ZIF-68 was 0.0001 μg·mL^{-1}. Compared with the reported method (Table 3), the samples analyzed included air, adhesives, and consumer products. The analytical methods employed were the cataluminescence (CTL) method, headspace gas chromatographic analysis, and gas chromatography-mass spectrometry. The detection limits ranged from 0.1 to 2 ppm. However, the proposed method had a significantly lower detection limit than the reported methods.

3.6 Test results of actual samples

According to the optimized extraction conditions (Table 1), the SPME probe prepared with ZIF-68 was used to determine the actual samples. The actual sample gas chromatogram is shown in Supplementary Information Figure S10.

The specific migration amount of vinyl acetate in food packaging film, EVA coating, and infusion bag (similar to FCMs) was investigated, and 10% ethanol, deionized water, and normal saline were used as simulants (Table 4). The migration condition was soaking at normal temperature for 7 days or at 40°C for 30 min to simulate the long- and short-term storage of food and the contact between normal saline and infusion bag during infusion.

For the three parallel determinations of each real sample, the specific migration of vinyl acetate for the 10% ethanol soaking solution was 0.059 μg·mL^{-1}, the recovery was 87.0 ± 6.0%, and the RSD was 6.9%. The specific migration of vinyl acetate for the deionized water immersion solution was 0.033 μg·mL^{-1}, the recovery was 105.2±0.8%, and the RSD was 3.5%. The specific migration of vinyl acetate for the physiological saline immersion solution was 0.005 μg·mL^{-1}, the recovery was 96.5±2.5%, and the RSD was 2.7%. The results show that the method had good accuracy and precision and can be used to determine the specific migration of vinyl acetate in FCMs.

4. Conclusion

A convenient screening method of SPME probe coating was established: the DVS method was used to screen various materials with the vinyl acetate target molecule as the atmosphere. The DVS results were consistent with the adsorption performance of the prepared SPME probe coatings, which indicates that under the tested conditions this material pre-screening and SPME performance prediction method was good for vinyl acetate. The adsorption mechanism was theoretically deliberated. The ESP distributions on the surface of the adsorption material and CDD during the adsorption process were analyzed via computational simulation. The adsorption energy was derived using the VASP calculation software based on the DFT algorithm and was consistent with the extraction efficacy of the SPME probe. Finally, an SPME probe based on ZIF-68 was selected to optimize the extraction conditions. The detection limit of the method was 0.0001 μg·mL^{-1}, and the RSD of five parallel tests was 7.6%, which show a good linear correlation and good repeatability. All standard recoveries were above 85%, and the RSD was less than 7%. The established method had reliable accuracy and precision.

Figure captions

Figure 1. Schematic illustration of the DVS-based screening strategy and SPME probe application.

(a), Schematic diagrams of the mutual verification of the two methods; (b), Condition optimization and application of the ZIF-68-coated SPME probe.

Figure 2. SEM photographs of ZIF-68 and ZIF-68-coated SPME probe.

1, ×2.00k (scale bar, 20.0 μm) of ZIF-68; 2, ×10.0k (scale bar, 5.0 μm) of ZIF-68; 3, exterior view of SPME probe; 4, cross-sectional view of SPME probe; a, coating; b, stainless-steel wire.

Figure 3. Powder XRD spectrogram of ZIF-68.

The black curve depicts the theoretically simulated XRD pattern, and the red curve depicts the XRD pattern of the synthesized ZIF-68.

Figure 4. Mutual validation of the two methods and investigation of promising candidate materials.

(a), Adsorption time curve of vinyl acetate (P/P0= 0.1) by DVS; (b), Comparison of adsorption capacities of different materials using the DVS method; (c), Comparison of the SPME effects of different materials using the probe method; (d) Further study on the extraction effect of the ZIF materials. Note: The above DVS and SPME data were all single measurement data. It should be pointed out that: 1) For DVS, we take the UiO-66-COOH randomly selected as an example for illustration, yielding a relative standard deviation (RSD) of 2.34% across 7 independent replicate measurements (the precision data were shown in Section 5.4 of the Supplementary Information); 2) For SPME, it had a precision similar to that of the actual samples in Table 4.

Figure 5. ESP distributions of vinyl acetate, MIL-MOFs, and ZIF-MOFs.

(a), the ESP distribution of vinyl acetate; (b–f), the ESP distributions of MIL-53 (Al), MIL-53(Al)-NH_2, ZIF-8, ZIF-68, and ZIF-70.

Figure 6. Adsorption energy andCharge transfer distribution of 5 materials.

(a), Adsorption energy of five materials; (b), Charge transfer distribution of ZIF-70 and ZIF-68; (c), Charge transfer distribution of ZIF-8; (d); Charge transfer distribution of MIL-53(Al) and MIL-53(Al)-NH_2.

Figure 7. Effect of various SPME conditions on the extraction efficiency.

(a), salt concentration; (b), extraction temperature; (c), agitation speed; (d), extraction time. Note: the error bar shows the standard deviation for triplicate extractions.

Tables

Table 1 Extraction experimental conditions

Project		Parameter
SPME extraction conditions	Salt concentration (%)	30
	Extraction temperature (°C)	10
	Agitation speed (rpm)	800
	Extraction time (min)	20
Sample volume/mL		5
Headspace volume/mL		15
Length of the probe exposure/cm		3.1
Probe exposure geometry		Suspended vertically in the headspace phase

Table 2 Linear range, correlation of determination, and limit of detection (LOD)

Analyte	Linear range ($\mu g \cdot mL^{-1}$)	The regression equation and Coefficient of determination (R^2)	LOD ($\mu g \cdot mL^{-1}$, 3S/N)	RSD (%, n=5)
Vinyl acetate	0.001–10	y = 2E-08x - 0.0106 R^2=1.00	0.0001	7.6

Table 3 Comparison of the limits of detection between the proposed methods and other works

Number	Analyte	Substrate	LOD		Analytical technique	Ref.
			Original text	Equal to		
1	Vinyl Acetate	Air	1.0 ppm	1.0 ppm	Cataluminescence (CTL) sensor using nanosized MgO as the sensing material	38
2	Vinyl Acetate	Polyvinyl acetate emulsion adhesive	0.63 $mg \cdot kg^{-1}$	0.63 ppm	Static Headspace-Gas Chromatography-Mass	39
3	Vinyl Acetate	Air	1.5 ppbv	0.0015 ppm (by volume)	Gas Chromatography-Mass	40
4	Vinyl Acetate	Consumer products	0.1-2 ppmw	0.1-2 ppm (by weight)	Headspace/Gas Chromatographic-FID	41
5	Vinyl Acetate	Air	0.1 ppm	0.1 ppm	Gas Chromatographic-FID	42
6	Vinyl acetate	Food contact materials	0.0001 $\mu g \cdot mL^{-1}$	0.0001 ppm	Solid-phase microextraction	This work

Table 4 Migration and recovery rate of vinyl acetate (n=3)

Sample	Simulated liquid	Migration conditions	Simulated concentration of vinyl acetate in liquid ($\mu g \cdot mL^{-1}$)	Specific migration amount ($mg \cdot kg^{-1}$)	Recovery (%)	RSD (%)
Food packaging film[a]	10% Ethyl alcohol	Room temperature soaking for 7 d	0.060	0.059	87.0±6.0	6.9

EVA coating[b]	Deionized water	40°C soaking for 30 min	0.033	0.033	105.2±0.8	3.5
Infusion bag[c]	Normal saline	40°C soaking for 30 min	0.005	0.005	96.5±2.5	2.7

[a]Recovery of spiked 0.12 μg·mL^{-1} vinyl acetate.

[b]Recovery of spiked 0.02 μg·mL^{-1} vinyl acetate.

[c]Recovery of spiked 0.012 μg·mL^{-1} vinyl acetate.

Supplementary Data

Figure 1. Not involved.

Figure 2. Not involved.

Figure 3's source data can be found in Supplementary Data 1.

Figure 4's source data can be found in "Figure 4(a), Figure 4(b), (c) & (d)" sheet of Supplementary Data 2.

Figure 5's source data can be found in Supplementary Data 3.

Figure 6. Not involved.

Figure 7's source data can be found in "Figure 7" sheet of Supplementary Data 2.

REFERENCES

1. (EC)No.1935/2004, On materials and articles intended to come into contact with food and repealing Directives 80/590/EEC and 89/109/EEC.
2. (EU) No 10/2011, On plastic materials and articles intended to come into contact with food.
3. Zhu, W. J., Jin, P. N., Yang, H. R., Li, F., Wang, C., Li, T. M., & Fan, J. (2023). A green extraction strategy for the detection of antioxidants in food simulants and beverages migrated from plastic packaging materials. *Food Chemistry*, *406,* Article 135060.
4. Xue, M. G., Chai, X. S., Li, X. D., & Chen, R. Q. (2019). Migration of organic contaminants into dry powdered food in paper packaging materials and the influencing factors. *Journal of Food Engineering*, *262*, 75-82.
5. Lerch, M., Nguyen, K. H., & Granby, K. (2022). Is the use of paper food contact materials treated with per- andpolyfluorinated alkyl substances safe for high-temperature applications? –Migration study in real food and food simulants. *Food Chemistry, 393*, 133375-133385.
6. Khoshakhlagh, A. H., Saberi, H. R., Kosowska, A. G., & Kumar, V. (2023). Respiratory functions and health risk assessment in inhalationalexposure to vinyl acetate in the process of carpet manufacturing usingMonte Carlo simulations. *Environmental Science and Pollution Research, 30*, 32560-32572.
7. https://www.iarc.who.int/
8. Jiao, P. R., Wang, X., Yan, J., Bao, F. W., & Su, G. S. (2015). Determination of Residual Amounts of Vinyl Acetate in Water-based Adhesives for Cigarettes by Headspace-GC. *PTCA(PATR B: CHEM*. ANAL.), *51*, 943-945.
9. Hoppe, M., de Voogt, P., & Franz, R. (2016). Identification and quantification of oligomers as potential migrants in plastics food contact materials with a focus in polycondensates — A review. *Trends in Food Science & Technology*, *50*, 118-130.
10. Cardama A. L., Sendón, R., Bustos, J., Nieto, M. T., Losada, P. P., & de Quiros, A. R. B. (2022). Food and beverage can coatings: A review on chemical analysis, migration, and risk assessment. *Comprehensive Reviews in Food Science and Food Safety*, *21*, 3558-3611.
11. Arthur, C. L., & Pawliszyn, J. (1990). Solid Phase Microextraction with Thermal Desorption Using Fused Silica Optical Fibers. *Analytical Chemistry*, *62*, 2145-2148.
12. Jiang, Q., Zhang, S. W., & Sun, M. (2023). Recent advances on graphene and graphene oxide as extraction materials in solid-phase (micro)extraction. *Trends in Analytical Chemistry*, *168*, Article 117283.
13. Delinska, K., Rakowska, P. W., & Kloskowski, A. (2021). Porous material-based sorbent coatings in solid-phase microextraction technique: Recent trends and future perspectives. *Trends in Analytical Chemistry*, *143*, Article 116386.
14. Cruz, J. C., Rosa, M. A., Mor´es, L., Carasek, E., de Souza Crippam J. A., Figueiredo, E. C., & Queiroz, M. E. C. (2022). Magnetic restricted-access carbon nanotubes for SPME to determine cannabinoids in plasma samples by UHPLC-MS/MS. *Analytica Chimica Acta*, *1226*, 340160-340170.
15. Feng, J. J., Feng, J. Q., Ji, X. P., Li, C.Y., Han, S., Sun, H.L., & Sun, M. (2021) Recent advances of covalent organic frameworks for solid-phase microextraction. *Trends in Analytical Chemistry*, *137*, Article 116208.
16. Fang, Y. Y., Zhou, F. Z., Zhang, Q., Deng, C., Wu, M. Y., Shen, H. S., Tang, Y., & Wang, Y. J. (2024). Hierarchical covalent organic framework hollow nanofibers-bonded stainless steel fiber for efficient solid phase microextraction. *Talanta*, *267*, Article 125223.

17. Shahhoseini, F., Azizi, A., & Bottaro, C. S. (2022). A critical evaluation of molecularly imprinted polymer (MIP) coatings in solid phase microextraction devices. *Trends in Analytical Chemistry*, *156,* Article 116695.
18. Chen, Y. M., Yu, Y., Wang, S. H., Han, J. J., Fan, M. G., Zhao, Y. P., Qiu, J. L.; Yang, X., Zhu, F., & Ouyang, G. F. (2024). Molecularly imprinted polymer sheathed mesoporous silica tube as SPME fiber coating for determination of tobacco-specific nitrosamines in water. *Science of the Total Environment*, *906*, Article 167655.
19. Sun, M., Li, C. Y., Feng, J. Q., Sun, H. L., Sun, M. X., Feng, Y., Ji, X. P., Han, S., & Feng, J. J.(2022). Development of aerogels in solid-phase extraction and microextraction. *Trends in Analytical Chemistry*, *146,* Article 116497.
20. Xin, X. B., Li, C. Y., Min, S., Guo, W. J., & Feng, J. J. (2024). Silver nanoparticle-functionalized melamine-formaldehyde aerogel for online in-tube solid-phase microextraction of polycyclic aromatic hydrocarbons followed by HPLC-DAD analysis. *Journal of Chromatography A*, *1719*, Article 464767.
21. Yavir, K., Konieczna, K., Marcinkowski, L., & Kloskowski, A. (2020). Ionic liquids in the microextraction techniques: The influence of ILs structure and properties. *Trends in Analytical Chemistry*, *130*, Article 115994.
22. Delinska, K., Machowski, G., & Kloskowski, A. (2022). Development of SPME fiber coatings with tunable porosity for physical confinement of ionic liquids as an extraction media. *Microchemical Journal*, *178*, Article 107392.
23. Hoskins, B. F., & Robson, R. (1989). Infinite Polymeric Frameworks Consisting of Three Dimensionally Linked Rod-like Segments. *Journal of the American Chemical Society*, *111*, 5962-5964.
24. Kaskel, S. (2017). The chemistry of metal–organic frameworks. Synthesis, characterization, and applications. *Angew. Chem. Int. Ed. 56,* 1425-1675.
25. Cui, X. Y., Gu, Z. Y., Jiang, D. Q., Li, Y., Wang, H. F., & Yan, X. P. (2009). In Situ Hydrothermal Growth of Metal-Organic Framework 199 Films on Stainless Steel Fibers for Solid-Phase Microextraction of Gaseous Benzene Homologues. *Analytical Chemistry*, *81*, 9771-9777.
26. Bautista, P. R., Fernández, I. P., Pasán, J., & Pino, V. (2016). Are metal-organic frameworks able to provide a new generation of solid-phase microextraction coatings? - A review. *Analytica Chimica Acta*, *939*, 26-41.
27. Gutiérrez-Serpa, A., Pacheco-Fernández, I., Pasán, J., & Pino, V. (2019), Metal–Organic Frameworks as Key Materials for Solid-Phase Microextraction Devices—A Review. *Separations, 6*, 1-29.
28. Mondal, S., Xu, J. Q., Chen, G. S., Huang, S. M., Huang, C. Y., & Yin, L. (2019). Solid-phase microextraction of antibiotics from fish muscle by using MIL-101(Cr)NH_2-polyacrylonitrile fiber and their identification by liquid chromatography-tandem mass spectrometry. *Analytica Chimica Acta*, *1047*, 62-70.
29. Bolat, S., Demir, S., Erer, H., Pelit, F., Dzingeleviciene, R., Ligor, T., Buszewski, B., & Pelit, L. (2024). MOF-801 based solid phase microextraction fiber for the monitoring of indoor BTEX pollution. *Journal of Hazardous Materials*, *466*, Article 133607.
30. Geerlings, P., De Proft, F.,& Langenaeker, W. (2003). Conceptual density functional theory. *Chemical Reviews*, *103*, 1793-1873.
31. Sharma, P., Bao, J. J., Truhlar, D. G., & Gagliardi, L. (2021). Multiconfiguration Pair-Density Functional Theory. *Annual Review of Physical Chemistry*, *72*, 541-564.
32. Niu, J. J., Li, Z. Y., Yang, H. J., Ye, C. W., Chen, C., Li, D., Xu, J., & Fan, L. (2016). A water resistant solid-phase microextraction fiber with high selectivity prepared by a metal organic framework with perfluorinated pores. *Journal of Chromatography A*, *1441*, 16-23.
33. Kresse, G., & Furthmüller, J. (1996). Efficiency of ab-initio total energy calculations for metals and semiconductors using a plane-wave basis set. *Computational Materials Science*, *6*, 15-50.
34. Wang, V., Xu, N., Liu, J.C., Tang, G., & Geng, W. T. (2021). VASPKIT: A user-friendly interface facilitating high-throughput computing and analysis using VASP code. *Computer Physics Communications*, *267*, Article 108033.
35. Humphrey, W., Dalke, A., & Schulten. K. (1996). VMD: Visual Molecular Dynamics. *Journal of Molecular Graphics and Modelling*, *14*, 33-38.
36. Momma, K. F., & Izumi, F. (2011). VESTA 3 for three-dimensional visualization of crystal, volumetric and morphology data. *Journal of Applied Crystallography*, *44*, 1272-1276.
37. Stavitski, E.; Pidko, E. A.; Couck, S. (2011). Complexity behind CO_2 Capture on NH_2-MIL-53(Al). *Langmuir.*, *27*, 3970-3976.
38. Wu, C. Chou., Cao, X. A., Wen, Q., Wang, Z. H., Gao, Q. q., Zhu, H. C.(2009) A vinyl acetate sensor based on cataluminescence on MgO nanoparticles. *Talanta, 79,* 1223-1227.
39. Ji, H. W., Liu, J., Ye, C., Wan, Q., Han, W., Wang, F., Yang J. G., & Yang, H. J. (2011). Determination of Residual Vinyl Acetate in Polyvinyl Acetate Emulsion Adhesives for Cigarettewith Static Headspace-Gas Chromatography-Mass Spectrometry. *Tobacco Science & Technology,11,* 32-35.
40. Sturaro, A., Parvoli, G., Doretti, L., Bancomina, C., Neonato, C. (1994). Gas chromatographic/mass spectrometric determination of vinyl acetate levels in air. *Journal of Mass Spectromtry, 29,* 575-577.
41. Gauthier, A., Behymer, W., Bare, J., Kramer, M., Barranco, W. T., Longtin, J. P., Borghoff, S., & Jaques, A. (2025). Measurement of vinyl acetate monomer in consumer productsand modeled estimates of consumer exposure, *Journal of Exposure Science & Environmental Epidemiology,* 35, 933-942.
42. Sidhu, K. S. (1981). Determination of vinyl acetate in air by gas chromatography. *Journal of Applied Toxicology, 6,* 300-302.

Acknowledgements

Author Contributions

Jiajia Niu: Writing – review & editing. Jichao Zhao: Software. Liqing Yue: Writing – original draft, Data curation. Wanchen Zang: Resources. Zhe Jin: Resources. Cuiliu Fu: Software. Chen Chen: Resources. Dong Li: Resources. Youliang Zhu: Data curation. Xiaojie Li: Acquired the data.

Data availability

All relevant data will be made available upon request.

Declaration of competing interest

No external funding was received. The authors declare that they have no known competing financial interests or personal relationships that could have appeared to influence the work reported in this paper.

Editor summary:

Selecting a coating adsorbent for solid-phase microextraction (SPME) with good compatibility for target molecules can be difficult, and testing methods for the vinyl acetate monomer, which is commonly used in the production of food contact materials, remain underexplored. Here, the authors propose an approach for assessing adsorption performance that combines dynamic vapor sorption and computational simulations, reporting ZIF-68 as an optimal coating material for the SPME testing of vinyl acetate and evaluating the monomer's specific migration in several ethylene vinyl acetate copolymer materials.

Peer review information:

Communications Chemistry thanks Hossein Kazemian and the other, anonymous, reviewer(s) for their contribution to the peer review of this work. A peer review file is available.

Compatibility?

DVS inlet valve
DVS outlet valve
Test chamber
30.0 ℃

Screening group (DVS)

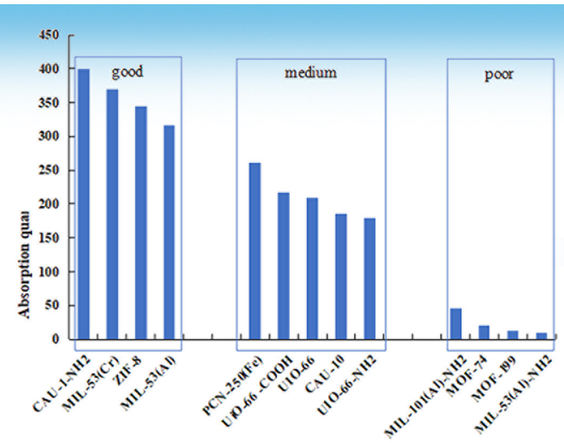

Coincidence

… …

Validation group (SPME probe)

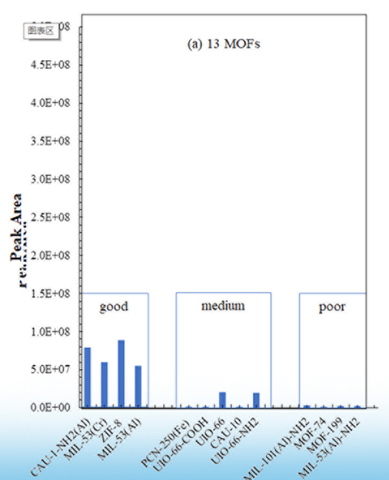

Adsorption materials

Vinyl acetate

Mechanism

Adsorption materials: ZIF-68

Target molecule: Vinyl acetate

Molecular association

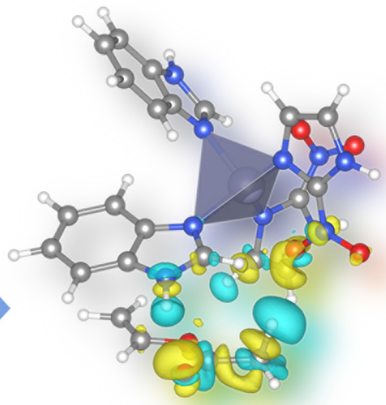

Adsorption energy: -50.7kJ/mol

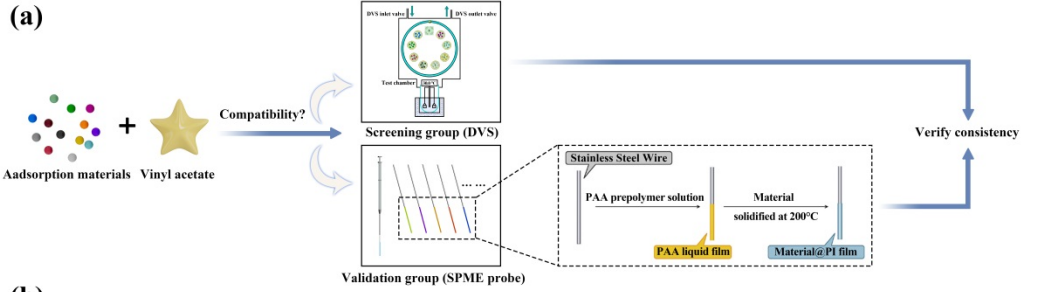

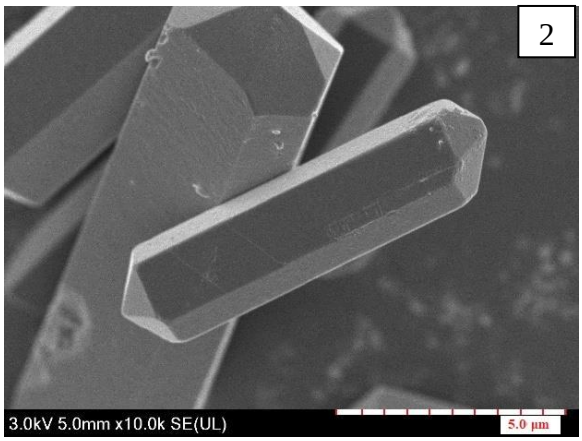

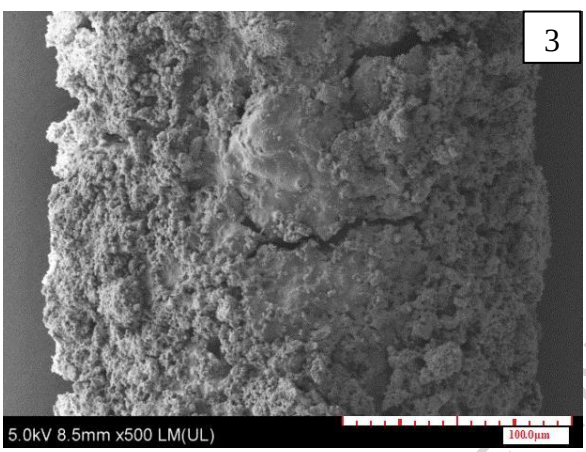

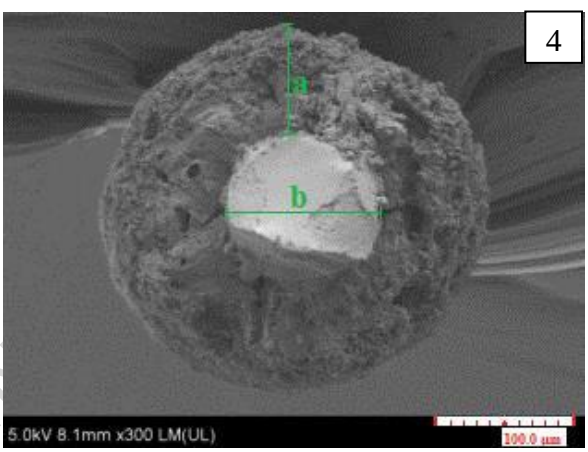

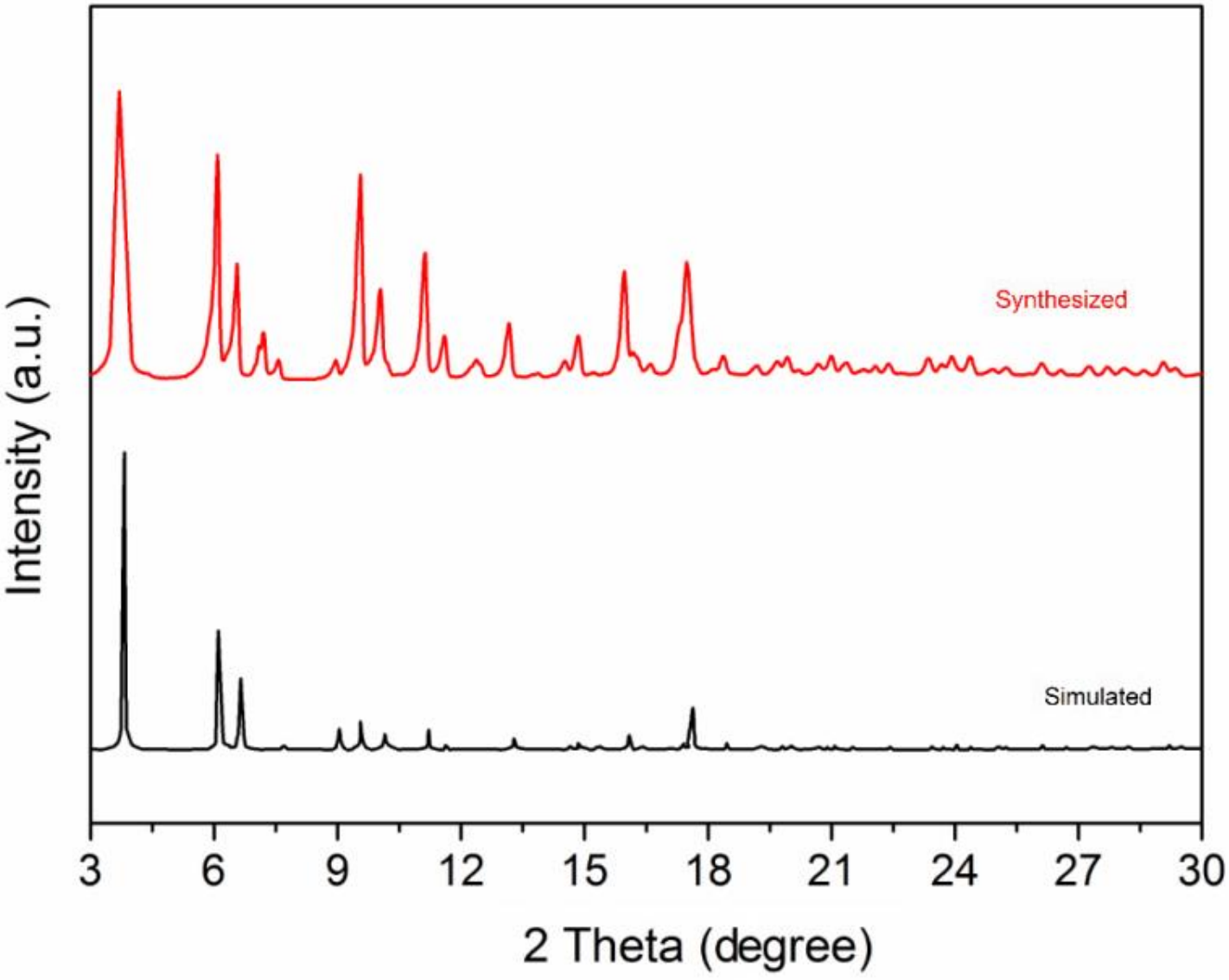

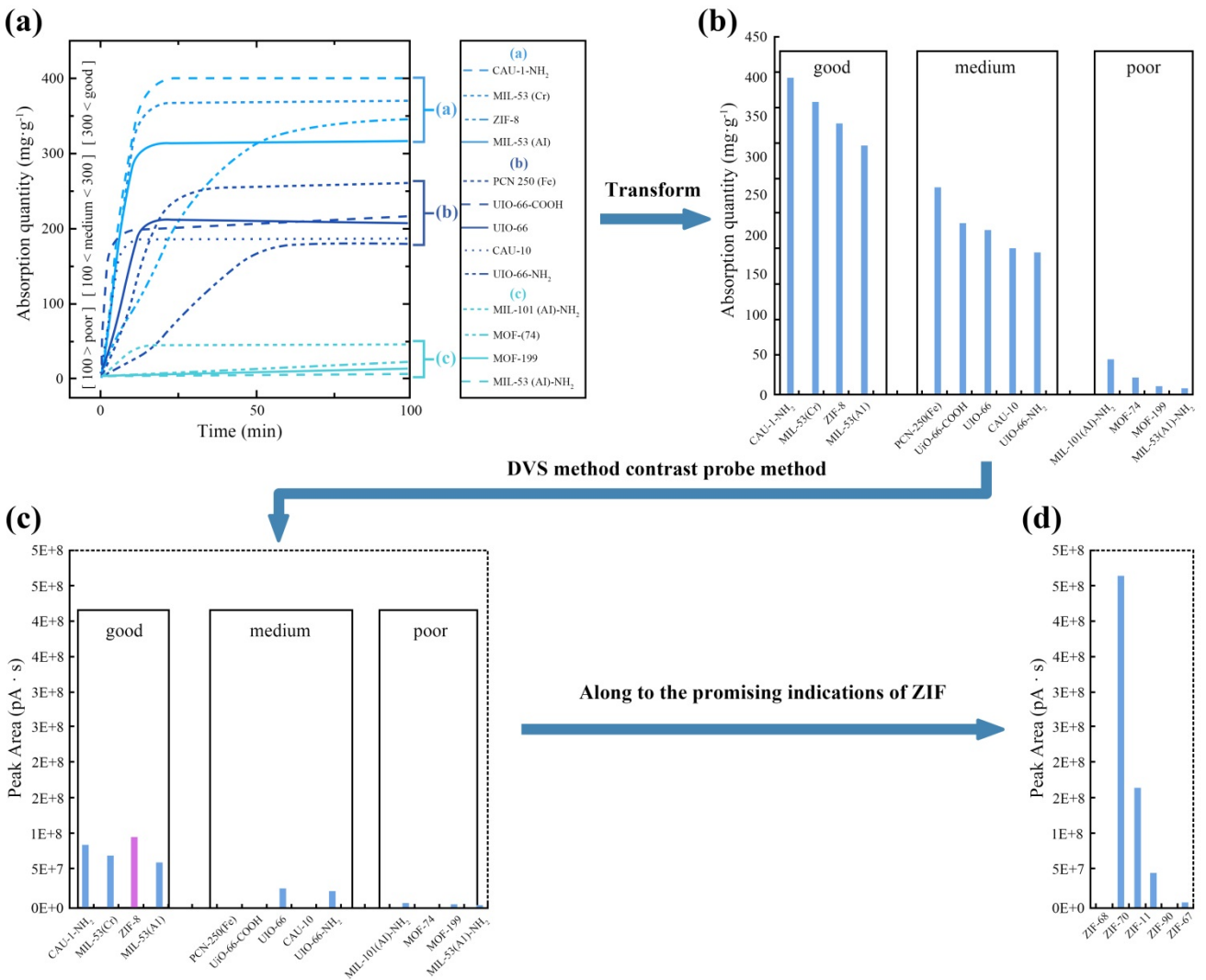
(a)
Absorption quantity (mg·g⁻¹)
[100 > poor] [100 < medium < 300] [300 < good]
Time (min)
(a)
CAU-1-NH2
MIL-53 (Cr)
ZIF-8
MIL-53 (AI)
(b)
PCN 250 (Fe)
UIO-66-COOH
UIO-66
CAU-10
UIO-66-NH2
(c)
MIL-101 (AI)-NH2
MOF-(74)
MOF-199
MIL-53 (AI)-NH2
Transform
(b)
good
medium
poor
Absorption quantity (mg·g⁻¹)
CAU-1-NH2
MIL-53(Cr)
ZIF-8
MIL-53(A1)
PCN-250(Fe)
UiO-66-COOH
UIO-66
CAU-10
UIO-66-NH2
MIL-101(AI)-NH2
MOF-74
MOF-199
MIL-53(A1)-NH2
DVS method contrast probe method
(c)
good
medium
poor
Peak Area (pA · s)
Along to the promising indications of ZIF
(d)
Peak Area (pA · s)
ZIF-68
ZIF-70
ZIF-11
ZIF-90
ZIF-67